12

Optoelectronic Circuits for Control of Lightwaves and Microwaves

Takahide Sakamoto
National Institute of Information and Communicantions Technology (currently, also with University of California, Davis)
Japan

1. Introduction

Interaction of lightwaves are very important, especially in the area of optical fiber communication and microwave photonic systems. Optical modulation and demodulation based on lasers, modulators, photodiodes, etc., have been intensively investigated, so far. As a result, so many optoelectronic devices have been matured enough to be practically used in real optical communication systems. Now, we are ready to explore novel functional optoelectronic circuits combining these devices as primary elements. In this chapter, we describe recent progress of the optoelectronic circuits, which enhances functionalities of optical fiber communication/ microwave photonic systems, introducing our latest results.
The first key word in this chapter is "data modulation/demodulation". Here, we describe novel optoelectronic circuits for advanced data modulation/demodulation. Our two approaches, multilevel signaling and spectral shaping, by the optoelectronic circuits are introduced. These technologies will be essentially useful to ultimately enhance spectral efficiency of the optical transmission systems, which is also applicable to microwave photonic systems.
Another keyword is "photonic oscillators." If we consider communication systems, in general, oscillators are very important as much as the data modulation/demodulation. In the transmitter side, optical carrier should be provided; in the receiver side, local oscillators should be prepared for the demodulation. Stable and precise, and flexible in some cases, oscillators are always required both for the optical fiber communication and microwave photonic systems. Here, we describe novel photonic oscillator technologies based on optoelectronic circuits, featuring our two key technologies: One is an optoelectronic oscillator circuits and the other is an optical comb generation circuits. By the circuits, multi-frequency carrier can be easily and stably generated, which would greatly simplify the parts of photonic oscillators in the optical communication/ microwave photonic systems.

2. Photonic oscillators, mixers

When we discuss nowadays photonic devices and components, it is a good idea to compare them with microwave components. Here, in this section, we briefly describe key photonic devices like photonic oscillators and mixers, which are really analogeous to microwave ones; we clarify the photonic circuits we discuss throughout in this chapter.

Laser sources are essential elements for optical communication, measurement and other technology, which plays important roles as an oscillator source at an optical frequency. Lasers have very high oscillation frequencies like Ĩ00 THz or higher, whereas microwave oscillators oscillates at H̃z - Ĩ00 GHz. Such high frequency oscillation characteristics of lasers offers several attractive applications. It allows synthesis or generation of ultrafast and wideband signals, like optical pulses and combs, which are applicable to test and measurements for investigating ultrafast phenomena. In addition, lightwaves generated from laser sources can be used as a carrier for data transmission in telecommunications, which is advantageous for large-capacity or ultra high-speed data transmissions because of its high-frequency oscillation characteristics. Huge capacity data transmission much beyond the capacity of radio-wave telecommunications have been reported, so far.

Laser as a photonic oscillator also offer another important features: they have good coherence as microwave oscillators do. This feature enables several useful applications in the area of measurements, signal synthesis, coherent communications and so on, which rely on interference of lightwaves. In general, it is not so easy to stabilize optical frequency and phases of lasers comparing with microwave oscillators. Recently, linewidth of semiconductor or fiber lasers are getting narrower in the order of kHz MHz, which accelerates progress of research and developement in this area.

To educe these great potential of photonic oscillators, we need to consider and devolope methods for interaction and control of lightwaves. For the purposes, mixers are commonly used in microwave technologies for mixing two signals to generate product of them. In photonic technologies, mixers should deal with interaction between lightwaves and between lightwaves and electrical signals (microwaves). Modulators and detectors are key elements as the photonic mixers. Modulators accepts input of lightwaves and electrical (microwave) signals, outputting their products at an optical frequency. Detectors, represented by photodetectors, are another important mixer, where an electrical signal is output as a mixing result of lightwaves.

Modulators are essential for shaping the sinusoidal optical carrier into a signal with a specific waveform and pulse shape. Intensity modulation technique has been investigated for long time to enable high-speed intensity modulation on lightwaves. Including direct modulation technique, several approaches have been investigated. Among them, currently, waveguide type modulators based on EO effects show promise owing to its capability of pure and ideal phase modulation. Modulation methods on amplitude, frequency and phase of lightwaves have been developed, which triggered, especially in telecom area, several types of modulation formats other than OOK. Vector modulation by IQ modulator is a powerful way to perform any modulation; thus the modulator is commonly used for advanced modulation in optical communications.

Demodulators (or detectors) are also important components for the interactions between light and microwaves. Photodiodes with PIN structure and avalanche-photodiodes at 10Gb/s or higher are now matured well, and balanced detection with the photodiodes are useful for coherent detection, with great sensitivity. Especially, a phase diversity is a powerful detection scheme to orthogonally demodulate phase and amplitude modulated lightwaves.

The modulators as a transmitter and photodiodes as a receiver are typical ways for the use in optical communication systems. However, we can explore more additional functions using the photonic mixers. Electrical or optical frequency conversion techniques allow the oscillators to generate sinusoidal signals at other frequencies. Linearly driven EOM upconverts baseband electrical signal to optical carrier frequency band, whereas, OE converter downconverts the signal over optical carrier to baseband by direct detection. IQ modulator enable vector modulation, orthogonal detection can vectorially downconverts signals.

Functions as harmonic mixing are also available by photonic mixers. Any nonlinearities in EO modulator or OE mixers cause nonlinear distortion to input signals. Electro-optic absorption in the EAMs and photocurrent in the PDs can be saturated for relatively large amplitude signals. The electro-optic effects in EO crystals easily generates higher order harmonics because of the nature of phase modulation characteristics. Nonlinearities in optical fiber or semiconductor materials are also useful for photonic mixing. Second-harmonic generation (SHG), four-wave-mixing (FWM) have been intensively investigated, eventually progressed and shows a promise for ultrafast or ultrawideband mixing process.

We know that there are many other important optical components and elements; optical fibers and fiber amplifiers are great technologies and other components such as optical filters, isolators, polarization controllers, AWG and so on are also important; however, they are not discussed in detail, here. Instead, we would like to state that the main subject of this chapter is to explore functional photonic circuits. To smoothly prompt the story of this chapter, we focus on the modified photonic oscillator structure consisting of EO and OE converters in its loop. This is a general form to deal with photonic oscillation and interaction with lightwaves and microwaves, and in some sense extension of photonic oscillators. In the loop, EO and OE converters (mixers) are involved. This configuration is a pair of OE/EO conversions if the electrical feedback is open. If the photocurrent detected in the PD is positively fed back to the EO mixer, this loop-structured circuit starts oscillation at a microwave frequency. This oscillator is called optoelectronic oscillator (OEO) and it has electrical and optical parts in its loop, thus good for dealing with interaction between lights and microwaves. The OEOs have been investigated in the context of ultra-stable microwave sources stabilization of mode-locked lasers, and so on. In this chapter, we discuss to modify the OEO to add functionality.

If the signal is down-converted to a baseband with a photo-mixer, the phase difference between the signal and local oscillator (LO) is detected and it can be used as a feedback signal. In this case, phase tracking operation is achieved with appropriate negative feedback. This loop is called a phase-locked loop (PLL). The PLL dealing with optical signal is called OPLL; there are basically two types of OPLL: one is for phase locking with optical carrier and the other is with optical clock. In general, the former one has a difficulty in phase tracking because laser stability is not good enough. On the other hand, challenges in the latter one is that we need to deal with high frequency or high clock-rated signals.

Although all of the topics related to the loop structure cannot be covered, this chapter picks up some. We know that advantage of the optical components and circuits are their wideband characteristics, while electronic circuits are advantageous for precise control and several functionalities for signal processing. Thus, the topics introduced here is, I believe, good examples to suitably use each of the merits. In the next sections, functional OEOs in special structures are described. In section 4, we discuss PLL structure, where ultrafast signal and its phase is controlled with low speed electronics. The topics in section 5 are regarding photonic harmonic mixers, which can extend the functionality of the photonic oscillators. In section 5, we describe ultraflat comb and ultrashort pulse generation from CW light and microwave signal.

3. Photoelectronic oscillator

Optoelectronic oscillators (OEOs) Yao & Maleki (1994) are very attractive devices for optical clock or subcarrier signal generation. OEO consists of an EO converter, and OE converter and feedback lines that connects the converters. In the circuit, EO- modulated lightwave by the EO converter is photodetected by the OE-converter; the photocurrent is fed back to the

EO converter again. If positive feedback gain is given enough, the circuits oscillates at the microwave frequency, in which electrical and optical signals are coverted with each other, exchanging their energy. If this gain is large enough to compensated for the loss in the OEO cavity, the OEO can be oscillated by using the energy of the pump light without supplying energy to the active components the OEO cavity.
The OEO has optical and electrical parts, which offers some interisting features different from optical or electrical oscillators. It has unique oscillation characteristics. For charactrization of oscillators, in general, it is a useful way to analyze transfer function, i.e. output power from the osillator measured against input power for pumping it. By this analysis, information of threshold, injection efficiency and other important basic characteristics can be obtained. Since the OEO has electrical and optical parts, it can output both electrical and optical signals for electrical or optical pumping; therefre, there are totally four input-output combnations for transfer functions.
Since the dimension of electrical and optical is different, the transfer function could be nonlinear. For example, the trace would have a shape of $y = \sqrt{x}$, if electrical output power is measured against optical pump power. If the transfer function has nonlinearity or wavelength (frequency) dependent characteristics, behavior of oscillation would be more complex, as discussed later. If we appropreately configure the OEO taking the nonlinear transfer funstions into acount, the OEO can oscillates even if feedback lines are paasive without gain blocks because, EO or OE converters can equivalently give positive gain. This feature is attravtive in some systems, ex. microwave photonic systems for remotrly distrobuting microwave or millimater signals without power supply at the remote places.
One of the important merits of the OEO is that such signals can be generated without any external microwave sources. Clock recovery or other functions useful for optical signal processing are easily obtained by this technology. Especially, in microwave or millimeter-wave photonic technologies, OEOs can play significant roles as photonic local oscillators. In addition, this configuration is advantageous for achieving ultra stable, low-phase-noise microwave sources because the optical fiber deployed in the optical part enables long cavity configuration which is known to be effective for decreasing intrinsic phase noise of the oscillator.
In this section, after brief description of principle of OEO, we describe OEO configurations for (1) single-mode oscillation, (2)wideband signal generation. In this section, we discuss to modify the OEO to add some useful fuctions, especially focusing on wideband signal generation. Once again, the oscilaltor has a distinctive hybrid structure consisting of electrical and optical parts. The optical part is suitable to deal with wideband signals. In electrical part, electrical functional components can be applied. If sufficient positive feedback gain is given to the components at a specific oscillation frequency f after one round trip, any functional components can be involved in the electrical and/or optical parts of the loop. For example, nonlinear components like frequency converter, harmonic generator, and other analog or digital circuits can be involved into the oscilaltor. Here, in this section, two cases are picked up as examples of modified OEOs: (1) bias-shift OEO and (2) harmonic OEO. The former one is effective to shift optical bias of the EO modulator deployed in the oscillator, which can generate optical two-tone signal. In the latter case, the oscillator consists of harmonic signal generator in its optical part, by which wideband optical signal like optical comb is generated by self oscillation.

3.1 Single-mode oscillation

In general, oscillators can oscillates at the multiple frequencies of cavity princeple mode. This phenomena is called multi-mode oscillation. Multi-mode oscillation is an easy way to obtain

a wideband comb-like signal, because generated signal has multiple frequency components with equal frequency spacing. However, mode competition observed in the multi-mode oscillators causes intensity fluctuation of the generated frequency components. The mode competition is originated by the use of one common gain medium in its cavity. In addition, phase relationship is not fixed and almost randomly varying because the oscillation of each frequency component is independent but slightly coupled with each other.

For a stable operation, single-mode oscillators are preferable, where the oscillators are allowed to oscillate at a single frequency. To achieve single-mode operation, positive feedback gain is selectively given to a particular oscillation mode of the cavity and to suppress undesired oscillation modes, as shown in Fig. **(a). Narrow-band filters or gain media can be utilized in the cavity for this purpose. In some gain media, the gain concentrates on the oscillated component after starting oscillation, which sometimes helps suppressing undesired components to be oscillated especially if the bandwidth of gain media or filter is not narrower enough comparing with FSR of the cavity.

OEO could be also operated either single or multi mode; the former is advantageous for stable operation. In the OEO, "single-mode" means the microwave cavity mode since the OEO is basically equivalent with a microwave oscillator. For the single-mode operation of the OEOs, there are two approaches to be taken. One is the approach, in which an microwave bandpass filter is applied in the electrical domain. High-Q narrowband filters at microwave frequency are available; for example, passband = 10 MHz, center frequency = 10 GHz, Q = 1000, etc.. The other approach is to adopt optical filtering in the optical domain. In this case, filtering should be applied the modulated lightwave. Thus, passband should be repeated Etalon resonator an suitable for the filters with periodical passband. The etalons cover the large FSR region, typically FSR= 10-1000 GHz, because of the difficulty in assembling long cavity structure. Optical disk cavities are also promising for the mode selection, which have a high Q characteristics. FSR of the disk filters is determined by its radius and reflective index of the material; typically FSR= 10GHz, Q = 1000. A loop filter consisting of an optical fiber is another candidate. Taking advantage of low-loss characteristics of optical fiber, the loop filter can exhibit ultra-high Q characteristics. Q = 100000, for example. On the other hand, FSR of the fiber-based loop filter is smaller, typically 10 100 MHz, since it cannot help having longer cavity length. This loop filter is sometimes called sub loop coupled with the main cavity. Challenging is to stabilize optical fiber isolating thermal effects to prevent frequency drift of the cavity.

Narrowband amplification in optical domain is also applicable to the mode selection in the OEO. Typical optical amplifiers based on stimulated emission, such as EDFA and SOA, have broad band width, which are not suitable for mode filtering in the OEO. Recently, it has been demonstrated to use a SBS based fiber amplifier for the mode selection. SBS is a nonlinear effects induced in optical fiber. The SBS gain bandwidth is very narrow, MHz. If the pump light is modulated at f_{pump}, the passband becomes multiple with the frequency separation of f_{pump}. Although it requires bulky setup, this method has some good points in terms of functionalities: (1) ultra narrow-passband effective for clear mode selection, (2) stable mode stability, (3) flexible tunability in oscillation frequency.

In the rest part of this section, another approach is discussed Sakamoto, Kawanishi, Shinada & Izutsu (2005). This filtering function can be commonized with resonant enhancement of optoelectronic effects. Filtering effects are mostly based on resonance, where the optical/electrical field can be enhanced at the resonant frequency. Eficiency of OE/EO conversions can be enhanced The SBS based OEO, mentioned above, is an example of such resonant enhancement obtained together with narrow filtering in the optical domain.

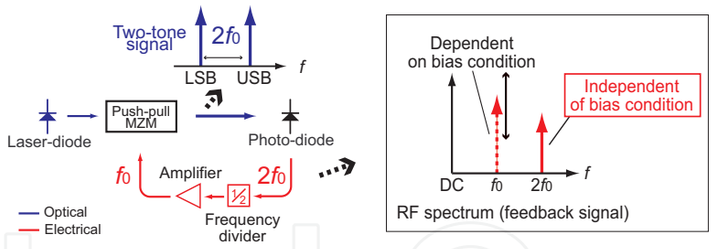

Fig. 1. Concept of two-tone signal generation using the proposed OEO.

Another example is shown in Fig. *, which called resonant-electrode-type OEO (RE-OEPO). In this case, EO- modulator for the EO conversion in the OEO is resonantly enhanced. Usually, electro-optic devices are designed for wideband operation, which covers from around DC to 10 GHz frequency range, aiming for high-speed baseband data modulation. On the other hand the EO components in the OEO could be operated only at/around the oscillation frequency, which allows alternative design approach. The modulator, elements of the OEO, has a resonant structure in the modulation electrode, so that its modulation bandwidth is limited but the modulation efficiency is improved. A standing wave arises if a sinusoidal signal is fed to the electrode. Note that the OEO can oscillate only at the frequency of the resonance without using any optical or RF filters, because the modulation efficiency out of the resonant frequency is suppressed. Therefore, single-mode operation is easily obtained. In addition, it is expected that the OEO made of such modulators oscillate with lower threshold power. This scheme can greatly reduce complexity and cost of OEOs.
Recently, several types of resonant enhancement is discussed in terms of high-efficient optical modulation. Disk type modulator constructed on silicon substrate is a good candidate, where modulator is fabricated over an optical ring resonator. Similar to the scheme, this resonant enhancement in the OE conversion would effectively increase the OEO feedback gain.

3.2 Two-tone signal generation

For electro-optic (EO) modulation implemented in such an OEO setup, a Mach-Zehnder modulator (MZM) is often used. Conventionally, the OEO usually generates a sinusoidal clock signal, *i.e.* an intensity-modulated double-sideband signal with a carrier in the frequency domain, where the MZM should be biased at or around the quadrature point. The MZM in the OEO has so far never been operated at or around the top/null bias conditions, which are $\frac{\pi}{2}$-shifted from the quadrature point, because feed back gain is intrinsically dismissed around these conditions. If the MZM can be biased at the null point, for instance, it is possible to generate an optical two-tone signal, *i.e.*, a carrier-suppressed dual-sideband signal, in the mode of self-oscillating operation. Such a two-tone signal is useful for distributing optical clocks to remote places because it exhibits good tolerance to the fading effect in dispersive fibers.
To overcome the limitation in the bias condition, a modified OEO configuration has been demonstrated, where the MZM can be operated at the bias conditions $\frac{\pi}{2}$-shifted from the quadrature point, Sakamoto, Kawanishi & Izutsu (2005). In the modified OEO, a feedback signal is extracted from optical beat between the upper-sideband (USB) and the lower-sideband (LSB) components of EO-modulated lightwave to achieve oscillation even if the MZM is biased at the top/null point. Figure 1 shows the basic concept of the proposed OEO. It consists of an MZM, a photodetector, a frequency divider, and an radio-frequency (RF) amplifier. The photodetector connected at the output of the modulator converts the modulation components into an RF signal. The frequency of the detected signal is divided

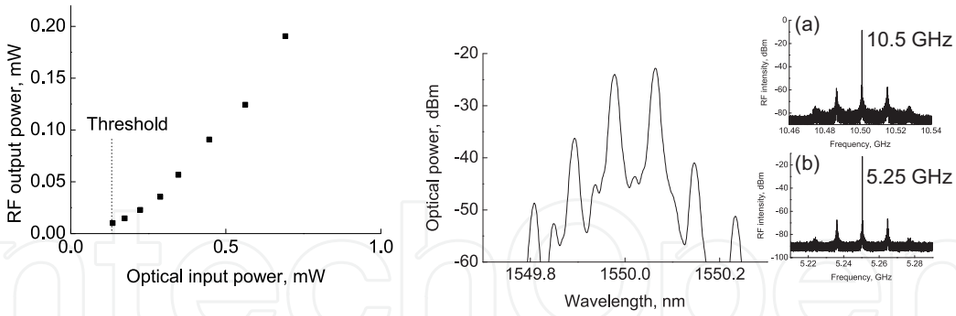

Fig. 2. (a) RF output power vs. optical input power. (b)Optical spectrum and RF spectra : (c) around 10.5 GHz, (d) around 5.25 GHz

in half by the frequency divider. The signal is amplified with the RF amplifier and positively fed back to the electrode of the modulator. If a lightwave with enough intensity is launched into the modulator, the loop gain of the oscillator becomes greater than one, and then the OEO starts oscillating. In this OEO, the oscillation frequency, f_0, is half the frequency of the optical beat between the USB and LSB components generated by the modulator. At the output of the photodetector, the photocurrent contains $2f_0$ frequency components, while the frequency of the driving signal at the MZM is f_0.

We explain here why the use of a frequency divider is essential in the $\frac{\pi}{2}$-shift bias operation. When the MZM is driven with a sinusoidal signal at repetition frequency f_0, the optical field of the EO-modulated lightwave is given as

$$E_{\text{out}} = \frac{1}{2}E_{\text{in}} \sum_{k=\infty}^{\infty} \left[J_k(A_1)\mathrm{e}^{jk\omega t+\theta_2} + J_k(A_2)\mathrm{e}^{jk\omega t+\theta_2} \right],$$

where E_{in} is the input field, and $J_k(\cdot)$ denotes the k-th order Bessel functions. The photocurrent of the direct-detected signal can be written as

$$i_{\text{ph}} = \frac{\eta|E_{\text{in}}|^2}{2} \left[1 + \cos\Delta\theta \left\{ J_0(\Delta A) + 2\sum_{k=1}^{\infty}(-1)^k J_{2k}(\Delta A)\cos 2k\omega t \right\} \right.$$
$$\left. - \sin\Delta\theta \left\{ 2\sum_{k=1}^{\infty}(-1)^k J_{2k-1}(\Delta A)\cos(2k-1)\omega t \right\} \right],$$

where η is the conversion efficiency of the photodiode. The amplitude of each mode at kf_0 is a sinusoidal function of bias V. It should be noted that the odd-order harmonic modes of the detected photo current are governed by sine functions, whereas the even-order modes are governed by cosine functions. In conventional OEOs, the fundamental mode at f_0 is fed back to the modulation electrode, where i_{ph} is maximized at the quadrature bias point ($\Delta\theta = \pm\frac{\pi}{2}$) but minimized at the zero/top-biased conditions. Therefore, less feedback gain is obtained in an OEO if the MZM is biased around the zero or top point. In the proposed OEO, on the other hand, the frequency divider divides the frequency in half so that the second-order mode is fed back to the modulation electrode. In this case, the feedback gain is minimized at the quadrature bias condition, $\Delta\theta = \frac{\pi}{2}$, and maximized at the zero/top bias conditions, $\Delta\theta = 0, \pm\pi$. An optical two-tone signal is generated by using the OEO employing an push-pull operated MZM biased at the null point.

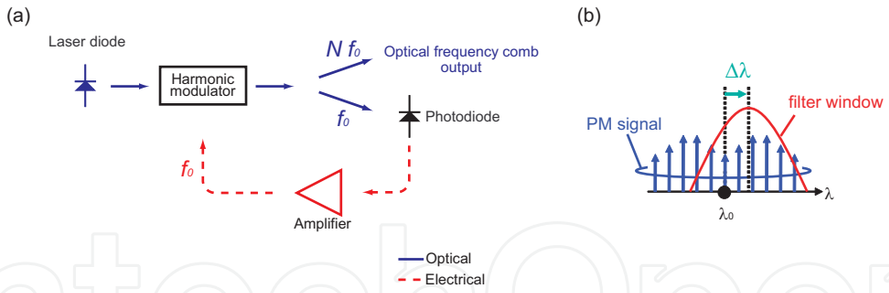

Fig. 3. (a) Concept of the OEO made of a harmonic modulator for optical frequency comb generation. (b) Offset filtering to convert phase-modulated lightwave to intensity-modulated feed-back signal.

Figure 2(a) shows threshold characteristics of the OEO, where RF output power is plotted against optical input power. Increasing the optical input power to the OEO, it started oscillating and the oscillation was stably maintained. The input power at the threshold for oscillation was 0.1 mW. The trace of the oscillation characteristics of the OEO is largely different from that of a conventional OEO. In our OEO output RF power is proportional to the square of the optical imput power, whereas conventional OEOs have square-root input-to-output transfer function. This is because the RF signal introduced back to the modulation electrode is clipped to a constant level by the frequency divider comprised of a logical counter. The optical input power does not change the feedback signal level; therefore, the output RF power is proportional to the square of the input power.
The optical output spectrum is shown in Fig. 2(b). An optical two-tone signal was successfully generated. The RF spectra before and frequency division are also shown in the inset of Fig. 2 (c)(d). The upper trace (c) indicates the spectrum of the signal at the input of the frequency divider. A 10.5-GHz single-tone spectrum was obtained there. The RF spectrum of the frequency-divided signal, which drives the modulator, is shown in the lower trace (d). In both spectra, side-mode suppression ratios were more than 50 dB, which can be improved by using a more appropriate BPF with a narrower frequency passband.
In this subsection, an optoelectronic oscillator employing a Mach-Zehnder modulator biased at the null/top conditions has been described, which is suitable for generating optical two-tone signals. Under the bias conditions, a frequency divider implemented in the OEO was crucial for extracting a feedback signal from the upper- and lower-sideband components of an electro-optic modulated lightwave.

3.3 Comb generation

Optical frequency comb generators can provide many attractive applications in micro-wave or millimeter-wave photonic technologiesJemison (2001): such as, optical frequency standard for absolute frequency measurement systems, local-oscillator remoting in radio-on-fiber systems, control of phased array antenna in radio astronomy systems, and so on.
Conventionally, a mode-locked laser is a popular candidate for such an optical frequency comb generation Arahira et al. (1994). Viewed from a practical perspective, however, the technology has difficulties in control of starting and keeping the state of mode-locking. This is because typical mode-locked lasers, consisting of multi-mode optical cavities, have multi stabilities in their operations. In this subsection, an OEO modified for comb generation is described: optoelectronic oscillator (OEO) made of a harmonic modulator is described. Sakamoto et al. (2006b)Sakamoto et al. (2007b)Sakamoto et al. (2006a)

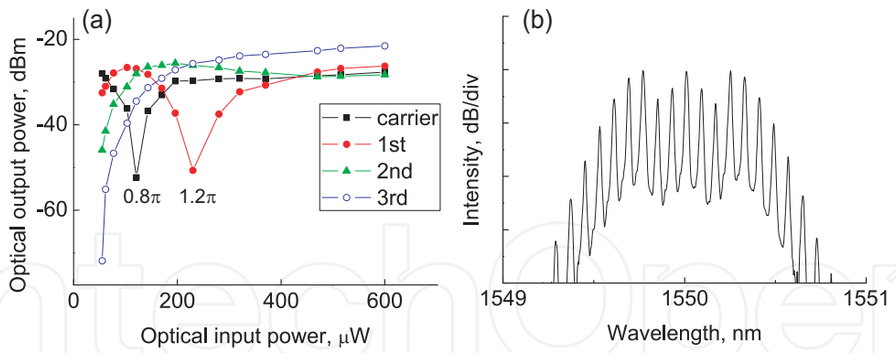

Fig. 4. (a) Optical intensity of each harmonic components against optical input power. Squares: at the carrier, dots: at the 1st-order, triangles: 2nd-order, circles: 3rd-order components. (b) Optical spectrum generated from the OEO (wavelength resolution = 0.01 nm).

It is known that EO modulation with larger amplitude signal promotes generating higher-order harmonics of the driving signal, obeying Bessel functions as discussed in the next section in detail. The OEO described in this subsection aims at the generation of frequency components higher than the oscillation frequency. In the OEO, an optical phase modulator is implemented in its oscillator cavity and driven by large-amplitude single-tone feed-back signal. Even this simple setup can generate multi-frequency components, i.e. optical frequency comb, with self oscillation as well as the conventional mode-locked lasers do. The most important difference from the mode-locking technologies is that the proposed comb generator is intrinsically a single-mode oscillator at a microwave frequency. Therefore, it is much more easy to start and maintain the oscillation comparing to the mode locking. A regenerative mode-locked laser is one of the successful examples of the wideband signal generation based on OEO structure, where a laser cavity is constructed in the optical part. However, it still relies on complex laser structure, whilw haronic-OEO has a single one-direction optical path structre without laser caivity.

Figure 3(a) shows the schematic diagram of the proposed OEO. The OEO consists of an optical harmonic modulator, a photodetector, and an RF amplifier. The harmonic modulator generates optical harmonic components of a modulation signal. The photodetector, connected at the output of the modulator, converts the fundamental modulation component (f_0) into an RF signal. The signal is amplified with the RF amplifier and led to the electrode of the modulator. If a lightwave with enough intensity is launched on the input of the harmonic modulator, the OEO starts oscillation because the fundamental modulation component at the frequency of f_0 is positively fed back to the modulator. Note that harmonic components (Nf_0) are generated at the output of the harmonic modulator, while the OEO is oscillating at f_0. Contrast to the conventional mode-locked lasers, the generated harmonics does not contribute to the oscillation, so that the OEO yields much more stable operation without complex control circuitry.

In this paper, an optical phase modulator is applied to the harmonic modulation in the OEO, where the modulator is driven by an RF signal with large amplitude. The modulator easily generates higher-order frequency components over the bandwidth of its modulation electrode. In order to achieve optoelectronic oscillation, it is required to detect feed back signal from the phase-modulated (PM) lightwave. For this purpose, we apply optical asymmetric filtering on the PM components, as shown in Fig. 3(b). By giving some frequency offset between the lightwave and the optical filter, the PM signal is converted into

intensity-modulated (IM) signal. This scheme is effective especially when the bandwidth of the filter is narrower than that of the PM signal. A fiber Bragg grating (FBG) is suitable for such an asymmetric filtering on deeply phase modulated signal since its stop band is typically narrower than the target bandwidth of frequency comb to be generated (100 GHz).
The OEO was made of an $LiNbO_3$ optical phase modulator, an optical coupler, an FBG, a photodiode (PD), an RF amplifier, a band-pass filter (BPF) and an RF delay line. The FBG had a 0.2-nm stop band and its Bragg wavelength was 1550.2 nm. The BPF determined the oscillation frequency of the OEO, and its center frequency and bandwidth of the BPF were 9.95 GHz and 10 MHz, respectively. The delay line aligned the loop length of the OEO to control the oscillation frequency, precisely. A CW light launched on the OEO was generated from a tunable laser diode (TLD). The center wavelength was aligned at 1550 nm, which was just near by the FBG stop band. The output lightwave from the FBG was photo-detected with the PD and introduced into the electrode of the phase modulator followed by the BPF and the amplifier. The harmonic modulated signal was tapped off with the optical coupler connected at the output of the modulator.
Increasing the optical power launched on the phase modulator, the OEO started oscillating. Fig. 4(a) shows optical output power of the phase-modulated components as a function of input power of the launched CW light. The squares, dots, triangles and circles indicate the 0th, 1st, 2nd and 3rd-order harmonic modulation components, respectively. As shown in Fig. 4(a), the input power at the threshold for oscillation was around 50 μW. Then, at the optical input power of 140 μW, we measured the optical spectrum of the generated signal. The output spectrum of the generated frequency obtained at (C) is shown in Fig.4 (b). Optical frequency comb with 120-GHz bandwidth and 9.95-GHz frequency spacing was successfully generated. The single-tone spectrum indicates that the OEO single-mode oscillated at the frequency of 9.95 GHz. The frequency spacing of the generated optical frequency comb was accurately controlled with a resolution of 30 kHz. By controlling the delay in the oscillator cavity, the oscillation frequency was continuously tuned within the passband of the BPF; the tuning range was about 10 MHz. The maximum phase-shift available in our experimental setup was restricted to about 1.7π [rad]. It is expected that more deep modulation using a high-power RF amplifier and/or a low-driving-voltage modulator would generate more wideband frequency comb.
In conclusion, in this subsection, an optoelectronic oscillator made of a $LiNbO_3$ phase modulator for self-oscillating frequency comb generation has been described. Deeply phase-modulated light was converted to intensity-modulated signal through asymmetric filtering by an FBG, and fed back to the modulator. Frequency comb generation with 120-GHz bandwidth and 9.95-GHz accurate frequency spacing was achieved. The frequency spacing of the comb signal was tunable in the range of 10 MHz with the resolution higher than 30 kHz. The comb generator was selfstarting single-mode oscillator and stable operation was easily achieved without complex control technique required for conventional mode-locked lasers.

4. Spectral enhancement and short pulse generation by photonic harmonic mixer

Generation of broadband comb and ultra short pulse train have been investigated for long time Margalit et al. (1998); Yokoyama et al. (2000); Yoshida & Nakazawa (1998); **?**); **?**); **?**); **?**); **?**); **?**. Especially in the last decade, compact and practical comb/pulse sources have been rapidly improved in the areas of test and measurements, optical telecommunications, and so on, accelerated by progress in semiconductor and fiber optics. For test and measurements, optical fiber mode-locked lasers based on passive mode-locking have been developed into compact packages, which can simply generate pulse train in femto-second region with a high

peak power of k - MWatt and a repetition rate of MHz or so Arahira et al. (1994). The technology is also useful for generation of ultra broadband optical comb that covers octave bandwidth. For telecomm use, active mode locked lasers and regenerative mode-locked lasers based on semiconductor or fiber laser structures have been intensively investigated, so far **???**. Optical combs generated from the sources have large frequency spacing and they can be utilized as multi-wavelength carriers for huge capacity transmission. They are also useful for ultra high-speed communications because the pulse train generated is in high repetition. For practical use, however, stabilization technique is inevitable for keeping mode-locked lasing operation. Flexible controllability and synchronization with external sources are also important issues.

Recently, approaches based on electro-optic (EO) synthesizing techniques are becoming increasingly attractive Kourogi et al. (1994). Behind this new trend, we know rapid progress in EO modulators like $LiNbO_3$- and semiconductor-based waveguide modulators with improved modulation bandwidth and decreased driving voltage Kondo et al. (2005); Sugiyama et al. (2002); Tsuzuki et al. (n.d.). In the approaches, wideband optical comb with a bandwith of several 100 GHz-THz and picosecond (or less) pulse train at a repetition of 10 100 GHz are generated from continuous-wave (CW) sources, which do not rely on any complex laser oscillation or cavity structures. This is of a great advantage for stable and flexible generation of optical comb/pulses.

In the former section, we described self-oscillating comb generation based on OEO configuration, where it is clarified that comb generation can be achieved without loosing features of single-mode oscillators. The modulator used in the harmonic OEO is phase modulator in that case. As discussed in the section, EO modulators are useful way for the comb generation because it is superior in stable and low-phase-noise operation. A difficulty remained is to flatly generate optical comb; in other words, it is difficult to generate optical comb which has frequency components with the equal intensity. In fact, with a use of a phase modulator the amplitude of each frequency component obeys Bessel's function in different order, thus we can see that the spectral profile is far from flat one. Looking at applications of the comb sources, it can be clearly understood why lack or weakness of any frequency components causes problems. If we consider to use the comb source in WDM systems, for example, each channel should has almost equivalent intensity; otherwise the channels with weak intensity has poor signal-to-ratio characteristics; the high-intensity channel suffers from nonlinear distortion through transmission. One of the possible ways to solve this problem is to apply an optical filter to the non-flat comb. However, this approach has some problems. To equalize and make the comb signal flat, the filter should have special transmittance profile. In addition, the efficiency of the comb generation would be worse because all components would be equalized to the intensity level of the weakest one.

In this section, we focus on this issue: flat comb generation by using electro-optic modulator, where a flat comb is generated by a combination of two phase-modulated non-flat comb signals. By this method, spectral ripples between the two phase-modulated lights are cancelled each other to form a flat spectral profile. An noticeable point of this method is that only single interferometric modulator is required for the operation. Another point is that the flat comb is generated from CW light and microwave sources, and no optical cavities are required.

First, in this section, flat comb generation and its theory is described. Four principle modes of operation are clarified, which are essential for the flat comb generation by two phase-modulated lights. Next, synthesis of optical pulse train from the flat comb is described. Spectral enhancement and/or pulse compression with an aid of nonlinear fiber is also discussed.

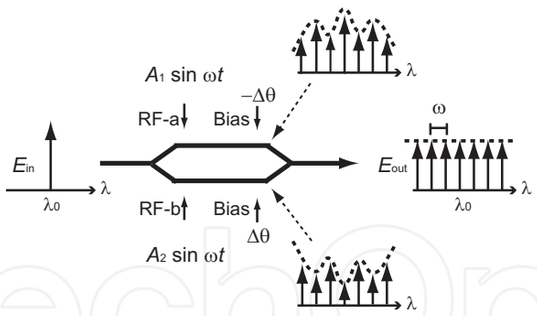

Fig. 5. Concept of ultraflat optical frequency comb generation using a conventional Mach-Zehnder modulator. A CW lightwave is EO modulated by a dual-drive Mach-Zehnder modulator driven with large sinusoidal signals with different amplitudes.

4.1 Ultra-flat comb generation

Fig. 5 shows the principle of flat comb generation by the combination of two phase modulated lightwaves Sakamoto et al. (2007a). In the optical frequency comb generator, an input continuous-wave (CW) lightwave is EO modulated with a large amplitude RF signal using a conventional MZM. Higher-order sideband frequency components (with respect to the input CW light) are generated. These components can be used as a frequency comb because the signal has a spectrum with a constant frequency spacing. Conventionally, however, the intensity of each component is highly dependent on the harmonic order. We will find, in this section, that the spectral unflatness can be cancelled if the dual arms of the MZM are driven by in-phase sinusoidal signals, RF-a and RF-b in Fig. 5, with a specific amplitude difference.

4.1.1 Principle opetation modes for flat comb generation

Here, in this subsection, principle operation modes for flatly generating optical comb using an MZM are analytically derived. Sakamoto et al. (2007a)

Suppose that the optical phase shift induced by signals RF-a and RF-b are $\Phi_a(t) = (\overline{A} + \Delta A)\sin(2\pi f_0 t + \Delta\phi_{\mathrm{ab}})$, $\Phi_b(t) = (\overline{A} - \Delta A)\sin(2\pi f_0 t - \Delta\phi_{\mathrm{ab}})$, respectively, where $\overline{A}$ is the average amplitude of the zero-to-peak phase shift induced by RF-a and Rf-b; $2\Delta A$ is difference between them; f_0 is the modulation frequency; $2\Delta\phi_{\mathrm{ab}}$ is the phase difference between RF-a and RF-b.

For large-amplitude driving signals, power conversion efficiency from the input CW light to each harmonic mode can be asymptotically approximated as

$$\begin{aligned}\eta_k &\equiv \frac{P_k}{P_{\mathrm{in}}} \\ &\approx \frac{1}{2\pi\overline{A}}\left|\mathrm{e}^{\mathrm{æ}(\Delta\theta+k\Delta\phi_{\mathrm{ab}})}\cos(\alpha+\Delta A)+\mathrm{e}^{-\mathrm{æ}(\Delta\theta+k\Delta\phi_{\mathrm{ab}})}\cos(\alpha-\Delta A)\right|^2 \\ &= \frac{1}{2\pi\overline{A}}\left[1+\cos(2\Delta A)\cos(2\Delta\theta+2k\Delta\phi_{\mathrm{ab}})+\cos(2\Delta A)\cos\beta\cos(k\pi)\right. \\ &\quad \left.+\cos(2\Delta\theta+2k\Delta\phi_{\mathrm{ab}})\cos\beta\cos(k\pi)\right] \qquad (1)\end{aligned}$$

, where $\beta \equiv \overline{A} - \frac{\pi}{2}(+\mathrm{Higher}-\mathrm{order\ term})$. This expression describes behavior of the generated comb well as long as $\overline{A}$ is large enough. Generally, the conversion efficiency is highly dependent on the harmonic order of the driving signal, k, which means that the frequency comb generated from the MZM has a non-flat spectrum.

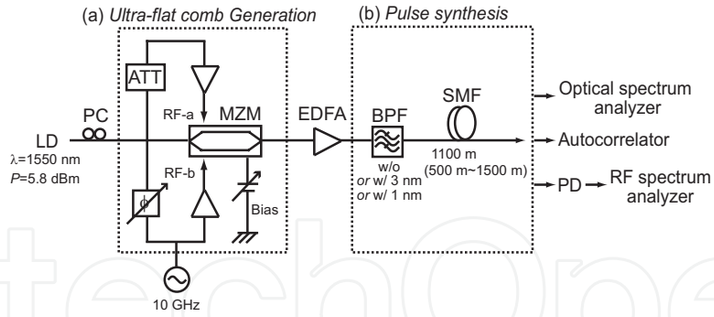

Fig. 6. Experimental setup; LD: laser diode, PC: polarization controller, MZM: Mach-Zehnder modulator, ATT: RF attenuator, EDFA: Erbium-doped fiber amplifier, BPF: optical bandpass filter, SMF: standard single-mode fiber, PD: photodiode.

To make the comb flat in the optical frequency domain, the intensity of each mode should be independent of k. From Eq. 1, the condition is

$$\cos(2\Delta A) + \cos\left(2\Delta\theta + 2k\Delta\phi_{\mathrm{ab}}\right) = 0 \tag{2}$$

To keep this equation for any k, the second term should be independent of k. $\Delta\phi_{\mathrm{ab}}$ should satisfy

$$\Delta\phi_{\mathrm{ab}} = 0 \text{ or } \pm\frac{\pi}{2}. \tag{3}$$

It should be noted that $\Delta\phi_{\mathrm{ab}} = 0$ and $\Delta\phi_{\mathrm{ab}} = \frac{\pi}{2}$ correspond to the cases of "in-phase" and "out-of-phase (push-pull)" driven conditions, respectively.
In the "in-phase" driven case ($\Delta\phi_{\mathrm{ab}} = 0$), the difference of the induced phase difference and bias difference should be related as

$$\Delta A \pm \Delta\theta = n\pi + \frac{\pi}{2}. \tag{4}$$

to make the spectral envelope flattened. Sakamoto et al. (2007a)
In the case of $\Delta\phi_{\mathrm{ab}} = \frac{\pi}{2}$, the MZM is allowed to be "out-of-phase (push-pull)" driven Sakamoto et al. (2011). From Eq. 2, the flat spectrum condition yields

$$\Delta A = \pm\frac{\pi}{4}, \Delta\theta = \pm\frac{\pi}{4} \tag{5}$$

From Eq. 4 and Eq. 5, it is found that there are conditions for flat frequency comb generation both for "in-phase" and "out-of-phase" driving cases, and the former condition is more robust since we only need to keep the balance between ΔA and $\Delta\theta$. If we make the efficiency of the generated comb maximum, however, the driving condition for "in-phase" driven case also results in $\Delta A = \pm\frac{\pi}{4}$, $\Delta\theta = \pm\frac{\pi}{4}$.

4.1.2 Experimental proof

Next, the flat spectrum condition in the four operation modes are experimentally proved. Fig. 6 shows the experimental setup, which is commonly referred in this chapter hereafter. The optical frequency comb generator consisted of a semiconductor laser diode (LD) and a $LiNbO_3$ dual-drive MZM having half-wave voltage of 5.4 V. A CW light was generated from the LD, whose center wavelength and intensity of the LD was 1550 nm and 5.8 dBm, respectively. The

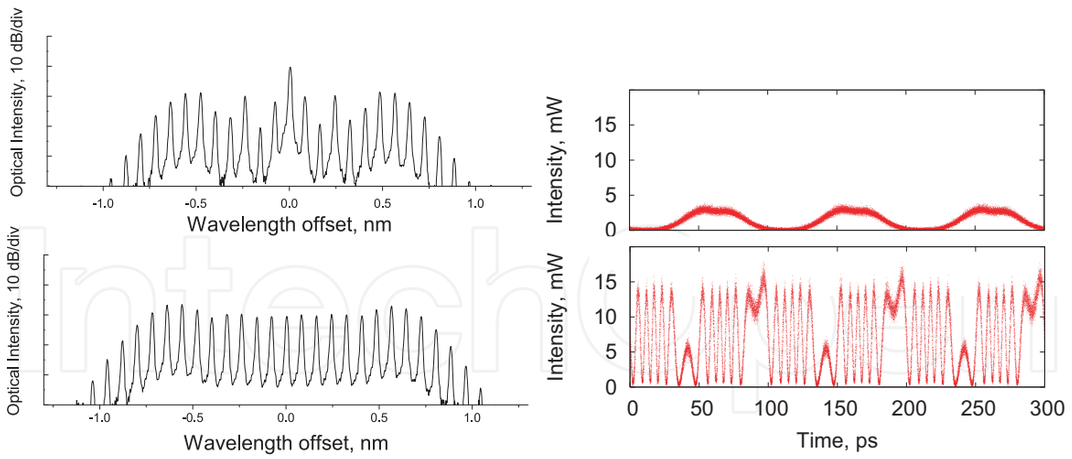

Fig. 7. Optical spectra; (a) Single-arm driven, (b) $\Delta_p hi = 0$ (in-phase), (c) $\Delta_p hi = 0.4\pi$, (d) $\Delta_p hi = 0$ (out-of-phase), Optical waveforms measured with an four-wave-mixing-based all-optical sampler (temporal resolution = 2 ps); (a) in-phase mode, (b) out-of-phase mode

CW light was introduced into the modulator through a polarization controller to maximize modulation efficiency. The MZM was dual-driven with sinusoidal signals with different amplitudes (RF-a, RF-b). The RF sinusoidal signal at a frequency of 10 GHz was generated from a synthesizer, divided in half with a hybrid coupler, amplified with microwave boosters, and then fed to each modulation electrode of the modulator. The intensity of RF-a injected into the electrode was attenuated a little by giving loss to the feeder line connected with the electrode. The input intensities of RF-a and RF-b were 35.9 dBm and 36.4 dBm, respectively Sakamoto et al. (2008). In order to select the operation modes, mechanically tunable delay line with tuning range over 100 ps was implemented in the feeder line for RF-a. The modulation spectra obtained from the frequency comb generator were measured with an optical spectrum analyzer. Optical waveform was measured with a four-wave-mixing-based all-optical sampler having temporal resolution of 2 ps.

Fig. 7 shows the optical spectra of the generated frequency comb. (a) is the case obtained when the MZM was driven in a single arm, where the driving condition was far from the "flat-spectrum" condition. (b) is the spectrum under the "flat-spectrum" condition in the "in-phase" operation mode. The delay between the RF-a and RF-b was set at 0 ($\Delta\phi_{\mathrm{ab}} = 0$). The RF power of the driving signals were 35.9 dBm and 36.4 dBm, respectively. Keeping the intensities of the driving signals, delay between RF-a and RF-b was detuned from $\Delta\phi_{\mathrm{ab}} = 0$. The spectral profile became asymmetric as shown in (c), where $\Delta\phi_{\mathrm{ab}} \approx 0.2\pi$. The spectrum became flat again when $\Delta\phi_{\mathrm{ab}} = \frac{\pi}{2}$ as shown in (d). The spectral at (b) and (d) were almost the same as expected and the 10-dB bandwidth was about 210 GHz in the experiments. Optical spectra with almost same the profile was monitored even when the optical bias condition was changed from the up-slope bias condition to the down-slope one. It has been confirmed that there are totally four different operation modes for flat comb generation using the MZM.

Characterization of the temporal waveform helps account for the behavior of the operation modes. Fig. 7 shows the optical waveforms measured with the all-optical sampler. Fig. 7(a) is the case obtained when the MZM was operated in the in-phase mode. The optical waveform was sinusoidal like since the optical amplitude is modulated within the range between 0 to π under the condition. On the other hand, Fig. 7(b) is measured at the push-pull operation mode. In this case, the temporal waveform was sharply folded back and forth and it is found that the optical amplitude was over swang far beyond the full-swing range of 0-π.

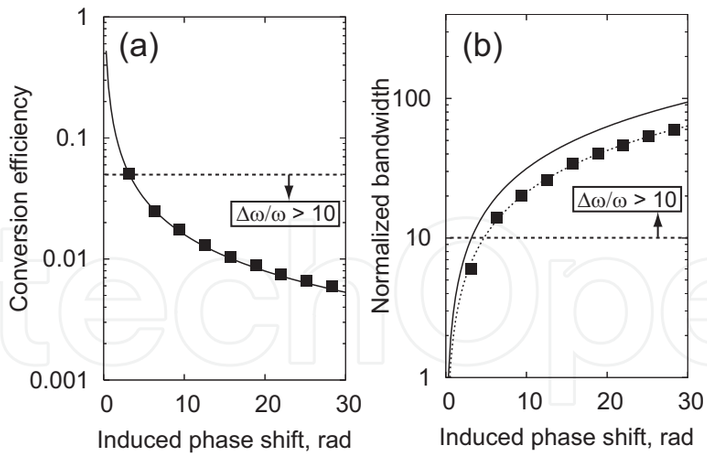

Fig. 8. (a) Maximum conversion efficiency, $\eta_{k,\max}$ vs. induced phase shift $\overline{A}$; theoretically (asymptotically) [solid line] and numerically averaged conversion efficiency within $0.5\Delta\omega$ [squares];(b) bandwidth, $\Delta\omega$, vs. $\overline{A}$; theoretically (asymptotically) ($\Delta\omega$)[solid line], number of CW components within 3-dB drop of η_k [squares], fitted curve ($0.67\Delta\omega$) [dashed line]; in each graph, the region of $\Delta\omega/\omega > 10$ is practically meaningful, where more than 10 frequency components are generated.

4.1.3 Characteristics of optical frequency comb generated from single-stage MZM

Here, primary characteristics of the generated comb are described providing with additional analysis. Conversion efficiency, bandwidth, noise characteristics are analyzed, in this subsection.

Conversion Efficiency

The output power should be maximized for higher efficient comb generation. Here, we discuss efficiency of comb generation. First, we define two parameters that stands for conversion efficiency of the comb geenration. One is a "total conversion efficiency", which is defined as the total output power from the modulator to the intensity of input CW light. The other is simply called "conversion effciency", which is defined as the intensity of individual frequency component to the input power.

Under the flat spectrum condition for "in-phase" mode, Eq. 3, the intrinsic conversion efficiency, excluding insertion loss due to impairment of the modulator and other extrincic loss, is theoretically derived from Eq. 1 and Eq. 4, resulting in

$$\eta_k = \frac{1-\cos 4\Delta\theta}{4\pi\overline{A}}, \tag{6}$$

which means that the conversion efficiency is maximized upto

$$\eta_{k,\max} = \frac{1}{2\pi\overline{A}}, \text{ when } \Delta A = \Delta\theta = \frac{\pi}{4}. \tag{7}$$

Note that this is the optimal driving condition for flatly generating an optical frequency comb with the maximum conversion efficiency. Hereafter, we call this equation the "maximum-efficiency condition" for ultraflat comb generation.

For the out-of-phase operation mode, the conversion efficiency yields,

$$\eta_{k,\mathrm{out-of-phase}} = \frac{1}{2\pi\overline{A}}, \tag{8}$$

, which is equivalent with the maximum-efficiency condition for the inphase operation mode, Eq. 7.
Fig. 8(a) shows the maximum conversion efficiency, $\eta_{k,\max}$ plotted against the average induced phase shift of $\overline{A}$. The solid curve indicates the theoretically derived conversion efficiency, Eq. 7 or 8. The squares in the plot indicate the numerically calculated average conversion efficiencies within the $0.5\Delta\omega$ bandwidth with respect to each value of $\overline{A}$. For the calculation, optical spectrum of the generated comb is calculated by using a First-Fourier-Transform (FFT) method, which is commonly used for spectral analysis of modulated lightwave. The range of $\overline{A}$ for the calculation is restricted in the rage of $\frac{\Delta\omega}{\omega} > 10$, where the generated comb has practically sufficient number of frequency components. The good agreement with numerical data proves that Eq. 7 or 8 is valid in the practical range.

Bandwidth

Bandwidth of the comb under the flat spectrum conditions is estimated, here. Under the flat spectrum conditions, energy is equally distributed to each frequency component of the generated comb. From the physical point of view, however, the finite number of the generated frequency comb is, obviously, allowed to have the same intensity in the spectrum; otherwise, total energy is diverged. The approximation for Eq. 1 is valid as long as $k << k_0$ and η_k rapidly approaches zero for $k >> k_0$. It is reasonable to assume that optical energy is equally distributed to each frequency mode around the center wavelength (i.e. $k << k_0$). Since the total energy, $\overline{P_{\mathrm{out}}}$, can be calculated in time domain, the bandwidth of the frequency comb becomes

$$\Delta\omega = \frac{\overline{P_{\mathrm{out}}}\omega}{\eta_k P_{\mathrm{in}}} \approx \pi\overline{A}\omega \ \ (\text{for small } \Delta A), \tag{9}$$

which is almost independent of ΔA (or $\Delta\theta$).
As for the comb generated under the out-of-phase operation mode, the analysis also results in the same bandwidth.
In Fig.8(b), the bandwidth, $\Delta\omega$ is plotted as a function of $\overline{A}$. In the graph, the solid curve indicates the theoretical bandwidth derived in Eq. 9; the squares represent the calculated 3-dB bandwidths required for keeping conversion efficiency of less than 3-dB rolling off from the center wavelength. These data almost lie on the fitted curve of $0.67\Delta\omega$, which is also plotted as a dashed curve in the graph. From this analysis, frequency components within 67% of the theoretical bandwidth of $\Delta\omega$ are numerically proven to have sufficient intensity with less than a 3-dB drop in the conversion efficiency. The 33% difference from the predicted $\Delta\omega$ is mainly because the shape of actual spectrum of the generated comb slightly differs from a rectangle assumed in the derivation of Eq. 7.

4.2 Linear pulse synthesis

Generation of picosecond optical pulse train at a high repetition rate **??????** has been extensively studied to achieve highly stable and flexible operation, aiming at the use in ultra-high-speed data transmission or in ultra-fast photonic measurement systems. Conventionally, actively/passively mode-locked lasers based on semiconductor or fiber-optic

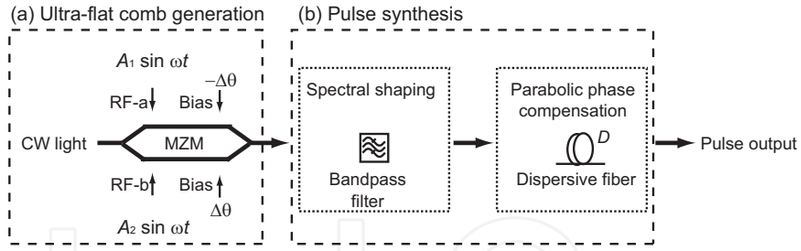

Fig. 9. Generation of ultra-short pulses by using a single-stage conventional Mach-Zehnder modulator.

technologies have been typically used to generate such pulse trains **???**. In the technologies, however, the laser cavity should be strictly designed and stabilized to generate stable pulse trains, which reduces flexibility in the operation. Especially, its repetition rate of the generated pulses is almost fixed and its scarce tunability has been provided. In addition, the highly nonlinear properties involved in generating pulses also restrict its operating conditions, which leads to limited output optical power and to uncontrollable chirp characteristics.

In the previous section, ultra-flat frequency comb generation by using only an MZM has been described. In this section, we apply it to generation of ultrafast pulse train. Basically, the strategy to synthesize optical pulse train from the comb source is as follows: (1) Phase differences between frequency components are aligned to be zero to form impulsive pulse train. (2) Profile of temporal waveform is controlled by spectral shaping to the generated comb.

By this approach, pulse trains with a pulse width of picosecond order can be obtained as discussed in this section. These two operations can be achieved in a linear process by simple passive components, as discussed in this section. The first one, phase comensation, is easily achieved by using a commonly used optical dispersive fiber. The second one, spectral shaping, is also achieved with a typical optical bandpass filter. Thin-film filters can be used for this puropose.

Figure 9 shows the basic construction of the picosecond pulse generator employing single-stage MZM. The pulse source consists of two sections: one for (a) comb generation and the other for (b) pulse synthesis. Section (a), consisting of a single-stage MZM, has a role to flatly generate a frequency comb. In this section, a continuous-wave (CW) light is EO modulated with the MZM, which is dual-driven by sinusoidal in-phase or out-of-phase signals having different amplitudes. Section (b), on the other hand, is comprised of an optical filter and a fiber, and it spectrally shapes the generated comb into a pulse train having a sync^2-like or a Gaussian-like temporal waveform.

The advantages of this pulse source are 1) the pulses are generated in an optically linear process, so that the optical level of the generated pulse is easily controlled; 2) the pulse source can be started up quickly without the need for complicated control procedures; 3) the repetition rate and the center wavelength of the generated pulse can be flexibly and quickly controlled; 4) the generated pulse train is highly stable due to the simple structure of the pulse generator and to the maturity of the components employed; 5) the pulse generator guarantees ultra-low timing jitter due to the high coherence of the generated comb.

Phase characteristics of comb

To clarify the phase characteristics of the generated comb, we modify Eq. 1 to look into higher-order terms of the output field, yielding

$$E_{\text{out}} = \frac{1}{2}E_{\text{in}} \sum_{k=-\infty}^{\infty} \left[J_k(A_1) e^{j(k\omega t+\theta_1)} + J_k(A_2) e^{j(k\omega t+\theta_2)} \right]$$
$$\approx \frac{E_0}{2}\sqrt{\frac{2}{\pi}}\overline{A}^{-\frac{1}{2}} \sum_{k=-\infty}^{\infty} \left\{ \cos\left(\overline{A} - \frac{(2k+1)\pi}{4} + \frac{4k^2-1^2}{8}\overline{A}^{-1} + \Delta A \right) e^{æ\Delta\theta} \right.$$
$$\left. \cos\left(\overline{A} - \frac{(2k+1)\pi}{4} + \frac{4k^2-1^2}{8}\overline{A}^{-1} - \Delta A \right) e^{-æ\Delta\theta} \right\} e^{æ(\overline{\theta}+k\omega t)}, \quad (10)$$

Since we have already derived the flat spectrum conditions, we substitute Eq. 3 and Eq. 4 into Eq. 10, respectively. Under the flat spectrum condition for in-phase and out-of-phase modes, respectively, the amplitude and the phase of the frequency modes can be approximated as

$$A_k = \frac{E_0 \sin(2\Delta\theta)}{\sqrt{2\pi\overline{A}}}, \Phi_k = \pm\frac{4k^2-1}{8\overline{A}}, \quad (11)$$

where those series higher than the fourth order series of Φ_k are neglected. It should be noted that the amplitude is independent of the harmonic order of the generated frequency components, k; the optical phases of the modes are related through a parabolic function of k. This equation is valid as long as $|k| << k_{\max} = \pi\overline{A}$ is satisfied.

Linear pulse synthesis by fiber-optic circuits

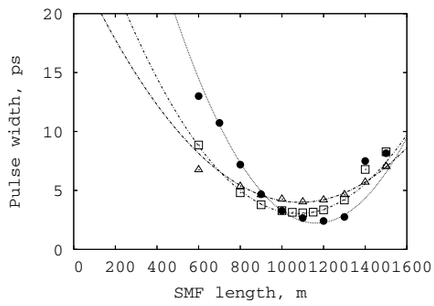

Fig. 10. Pulse width measured as a function of SMF length; solids: w/o filter, squares: w/ 3-nm filter, triangles: w/ 1-nm filter

Next, it is explained how the generated ultra-flat frequency comb is shaped into an ultra-short pulse train in section (b) of the pulse source by using Fourier spectral synthesis. In the case of in-phase operation mode, the story becomes more simple. From Eq. 11, it is found that the optical phase relationship between each mode is in a parabolic function of the mode number. Note that phase compensation with $-\Phi_k$ makes the temporal waveform of the generated comb impulsive. Such a phase compensation can be easily achieved by using a piece of standard optical fiber that gives a parabolic phase shift, i.e., a counter group delay, to the generated comb. The optimal length for the pulse generation is simply obtained as,

$$L = \mp\frac{\partial^2\Phi_k}{\partial k^2}(\beta_2\omega_0^2)^{-1} = \mp(\beta_2\overline{A}\omega_0^2)^{-1}, \quad (12)$$

where β_2 denotes group velocity dispersion in the fiber.

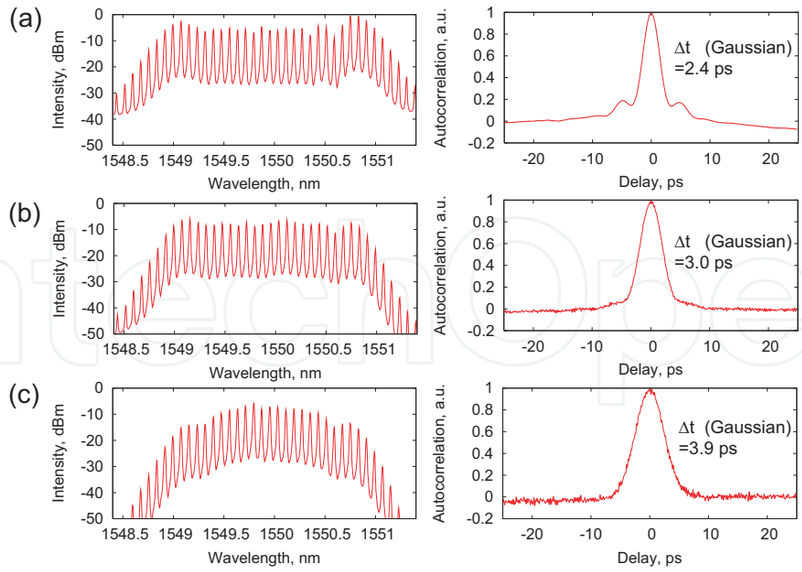

Fig. 11. Optical spectra (left side) and autocorrelation traces (right side); (a) W/o filtering, (b) sync^2-like shape, (c) Gaussian-like shape.

The synthesized pulse train, however, has a rather temporal waveform of the sync^2 function causing a large pedestal around the main pulse, because the generated comb has a rectangular spectrum. In many cases, it is required to shape the temporal waveform of the pulse into Gaussian to suppress the undesired pedestal. If an optical bandpass filter (OBPF) is applied to the generated comb having a cut-off frequency of $f << \frac{1}{2\pi} k_{\max} \omega$, the spectral envelope is shaped into the passband profile of the OBPF; thus, the temporal waveform should be a Fourier transform of the filter passband profile. For instance, if a Gaussian filter is applied to the generated comb together with the appropriate phase compensation of $-\Phi_k$, it is possible to generate Fourier-transform limited Gaussian pulse train with a pulse width of $T = 0.44/f$ and with a repetition of $T_0 = \frac{2\pi}{\omega}$. From this analysis, it is found that the optical pulses can be generated only using linear fiber-optic components. This has numerous practical advantages.

Experimental proof

Figure 6 shows the experimental setup for picosecond pulse generation using a single-stage MZM. In section (a) of the setup, an ultra-flat frequency comb was generated. A CW light was generated from a laser diode (LD), whose center wavelength and intensity were 1550 nm and 5.8 dBm, respectively. The CW light was introduced into the conventional $LiNbO_3$ dual-drive MZM that was driven under the flat spectrum condition. The MZM, having half-wave voltage of 5.4 V, was dual-driven with 10-GHz sinusoidal signals of RF-a and RF-b. The RF signals were generated from a synthesizer, divided in half with a hybrid coupler, amplified with microwave boosters, and fed into the electrodes of the modulator. The intensity of the RF-a fed into the electrode was attenuated a little by giving loss to the feeder line connected with the electrode. The average input intensity of RF-a and of RF-b was 38.5 dBm, and the difference between them was 1.0 dB. The average zero-to-peak deviation in the phase shift induced in the modulator was estimated to be 4.3 π. The phase difference between RF-a and RF-b was aligned to be zero by using a mechanically tunable delay line placed in the feeder cable for RF-a.

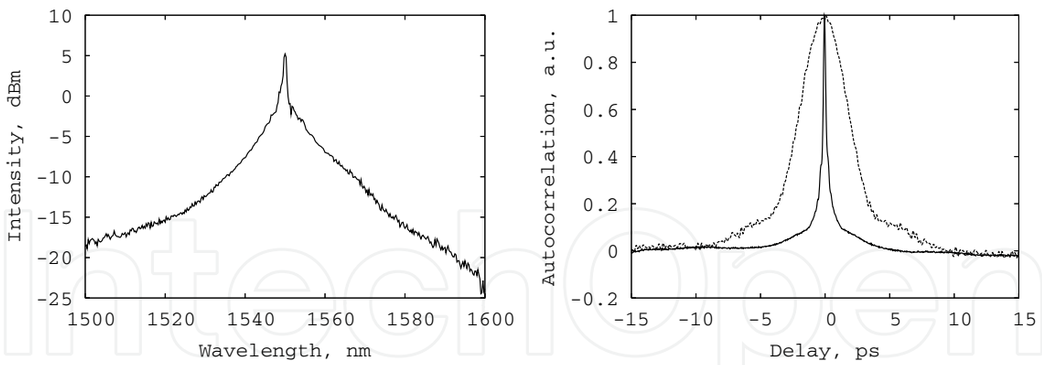

Fig. 12. Characteristics of generated pulse train; (a) optical spectrum , (b) autocorrelation traces, dotted: seed pulse, solid: compressed pulse

In section (b) of the experimental setup, the generated comb was converted into a pulse train. The comb was amplified with an Erbium-doped fiber amplifier (EDFA), and led to an optical thin-film band-pass filter (OBPF) followed by a piece of standard single-mode fiber (SMF). In addition to the function of the spectral shaping, the OBPF filtered out ASE noise generated from the EDFA. The characteristics of the generated pulse train were evaluated with an optical spectrum analyzer and an autocorrelator, and the timing jitter was analyzed with an RF spectrum analyzer.

First, in this experiment, the length of the SMF was optimized by evaluating evolution of the pulses through the fiber. Figure 10 shows pulse width dependence measured as a function of the SMF length. The pulse width was estimated from the autocorrelation traces assuming the Gaussian waveform. The circles, squares and triangles in the graph correspond to pulse widths measured (a) without a filter, (b) with a 3-nm filter ($\Delta\lambda_{\mathrm{bpf}} = 3$ nm) and (c) with a 1-nm filter ($\Delta\lambda_{\mathrm{bpf}} = 1$ nm). We found that $\tilde{1}100$ m is the optimal length for the pulse synthesis, where a group delay of 22 $\mathrm{ps}^2/\mathrm{nm}$ was introduced. Thus, the experimentally optimized length of the SMF is in good agreement with the theoretical value estimated from Eq. 12.

Figure 11 shows the optical spectra and the autocorrelation traces of the generated pulse trains. The narrowest pulse was obtained without using the OBPF, where the pulse width was estimated to be 2.4 ps. In this case, however, the pulse train had a large pedestal around the mainlobe of the pulse. For $\Delta\lambda_{\mathrm{bpf}} = 3$ nm, the temporal waveform was a sync^2-like function since the shape of the spectral envelope was square. The estimated pulse width was 3.0-ps. In the case of $\Delta\lambda_{\mathrm{bpf}} = 1$ nm, which is narrower than the spectral width of the generated comb, the optical spectrum had almost the same shape as the passband of the OBPF. It is confirmed that a Gaussian-like pulse train with a pulse width of 3.9 ps was generated, where time-bandwidth product was 0.45. The root-mean-square timing jitter evaluated from the single-sideband phase noise was as low as 130 fs, which almost reached the synthesizer's limit of the driving signal fed to the MZM. The generated pulse was greatly stable in long term, maintaining its waveform for at least a couple of hours.

In conclusion, we have proposed and demonstrated picosecond pulse generation using a conventional MZM. A 10-GHz, 2.4-ps pulse train was generated with $<$ 130-fs timing jitter. The pulse source is potentially more stable and more agile than conventional mode-locked lasers, and the setup is much simpler.

4.3 Nonlinear spectrum enhancement/ pulse compression

Femotosecond or sub-picosecond pulse train at GHz or higher repetition is promising for ultra-high speed optical transmissions and ultrafast photonic measurements. To generate such a short pulse train at high repetition rate, it is effective to use pulse compression technique together with a picosecond seed pulse source. As previously described, MZM-FCG based pulse source can simply and stably generate a picosecond pulse train. Here, we describe generation of 500-fs pulse train at repetition of 10 GHz using a conventional $LiNbO_3$ MZM, where compression ratio from driving RF signal reached 100 Morohashi et al. (2008) Morohashi et al. (2009). The generated pulse train exhibits great stability and ultra-low phase noise almost same the level as the synthesizer limit.

Among the pulse compression technologies, adiabatic soliton compression gathers great attention because of its easiness for handling, where a pulse train adiabatically evolves into shorter one in a dispersion decreasing fiber (DDF), keeping the fundamental soliton condition. In the adiabatic soliton compression using DDF, the compression ratio is proportional to the ratio of group velocity dispersion around input and output regions of the DDF. The pulse width of the seed pulse launched into the DDF should be ps to achieve generation of femtosecond or sub-picosecond pulse train because the compression ratio available in the DDF is typically 10 100.

For the soliton compression technique, we should keep soliton parameter defined as follows, as 1

$$N = \sqrt{\frac{\gamma P_0 T_0^2}{|\beta_2|}}. \tag{13}$$

Since the comb generated from the MZM-FCG has a bandwidth derived as Eq. 9, pulse width should be

$$T_{\mathrm{FWHM}} = \frac{2c}{\overline{A}\omega}, \tag{14}$$

where c is a constant in the order of 1 10.

Therefore, average power of the pulse train launched into the DDF results in

$$P_{\mathrm{ave}} = \frac{\omega T_{\mathrm{FWHM}} P_0}{2\pi} = \frac{\beta_2 \omega^3 \overline{A}^2}{2\pi\gamma 4c^2}, \tag{15}$$

which is a practical parameter for designing the compression stage.

Experimental setup is common as Fig. 6, but it has extended stage for nonlinear compression. In this stage, the generated pulse train is converted into femtosecond pulses using the adiabatic soliton compression technique. The picosecond pulse was amplified with an EDFA upto the average power of ** dBm; introduced into a dispersion-flattened dispersion decreasing fiber with the length of 1 km. In the fiber, wavelength dispersion was gradually decreased along the fiber from ** ps/nm/km to **ps/nm/km (estimated), and that was flattened enough in the wavelength range of ** nm to **nm. Autocorrelation traces are shown in Fig. 3. (a) is the trace measured at the output of the seed pulse generator (at point (A) inFig. 1). The half width of the suming Sech2 waveform, the pulse width of the seed pulse is estimated to be 2 ps; the pulse was compressed into 500-fs pulse train using DF-DDF.

From this experiments, it is shown that an ultrashort pulse train in femtosecond order can be generated from a CW light. This femtosecond pulse train also inherits the features of

Conditions	RF driving signals ($V_1 \sin\omega t, V_2 \sin\omega t$)	(Single-arm) bias voltage (V_{bias})	Conversion efficiency (η_k)	Normalized bandwidth ($\frac{\Delta\omega}{\omega}$)
Flat spectrum condition	$\left(\overline{V} \pm \frac{V_\pi}{2} \mp \frac{V_{\text{bias}}}{2}\right) \sin\omega t$	V_{bias}	$\frac{V_\pi\left[1-\cos\left(\frac{2\pi V_{\text{bias}}}{V_\pi}\right)\right]}{4\pi^2\overline{V}}$	$\pi^2 \frac{\overline{V}}{V_\pi}$
Maximum-efficiency condition	$\left(\overline{V} \pm \frac{V_\pi}{4}\right) \sin\omega t$	$\frac{V_\pi}{2}$	$\frac{V_\pi}{2\pi^2\overline{V}}$	$\pi^2 \frac{\overline{V}}{V_\pi}$

Table 1. Formulas for ultraflat frequency comb generation using MZM; $\overline{V} \equiv \frac{V_1+V_2}{2}$, where V_1, V_2 are zero-to-peak voltages of RF-a and RF-b, respectively, V_{bias}: bias voltage applied to one arm, V_π: half-wave voltage of the MZM.

linearly synthesized picosecond one: great stability, low-jitter characteristics, flex tunabilty in wavelength, repetition and so on.

4.4 Formulas for the flat comb and short pulse generation

We have reviewed techniques for generation of optical comb and pulses from CW source, focusing on the MZM-FCG based method, so far, Here, we summarize the operation modes and conditions required for obtaining the signals.

For flat comb generation, we have four operation modes. For both driving cases, the maximum conversion efficiency yields $\eta_k = \frac{1}{2\pi\overline{A}}$, which means that "in-phase" and "out-of-phase" driving modes can be effectively used with the same conversion efficiency. It is practically reasonable to operate the comb generator under the condition of the maximum conversion efficiency. By careful look at the signs of ΔA and $\Delta\theta$, it is found that the MZM can be biased at the quadrature point in the up slope or down slope of its transfer function.

By the combination of polarities of the driving signal and the bias condition, the MZM can be driven in totally four different principle operation modes, summarized as follows:

(1) Up-slope biased in-phase driven mode: $|\Delta\phi_{\text{ab}}| = 0$, $\Delta A = \pm\frac{\pi}{4}$, $\Delta\theta = \pm\frac{\pi}{4}$,

(2) Down-slope biased in-phase driven mode: $|\Delta\phi_{\text{ab}}| = 0$, $\Delta A = \pm\frac{\pi}{4}$, $\Delta\theta = \mp\frac{\pi}{4}$,

(3) Up-slope biased out-of-phase (push-pull) driven mode: $|\Delta\phi_{\text{ab}}| = \frac{\pi}{2}$, $\Delta A = \pm\frac{\pi}{4}$, $\Delta\theta = \pm\frac{\pi}{4}$,

(4) Down-slope biased out-of-phase (push-pull) driven mode: $|\Delta\phi_{\text{ab}}| = \frac{\pi}{2}$, $\Delta A = \pm\frac{\pi}{4}$, $\Delta\theta = \mp\frac{\pi}{4}$.

In-phase mode is suitable for short pulse generation because the generated pulse has smooth temporal waveform envelope and continuous phase characteristics. For picosecond pulse generation, a dispersive fiber with a length of $(|\beta_2|\overline{A}\omega_0^2)^{-1}$ [m] converts comb signal to pulse train with a pulse width of $2c/(\overline{A}\omega)$ [sec].

To obtain femtosecond pulses, the comb with average input power of $(\beta_2\omega^3\overline{A}^2)/(2\pi\gamma 4c^2)$ [W], should be launched into the DDF having following parameters: group velocity dispersions at input and output region, $\beta_{2,\text{in}}$, $\beta_{2,\text{out}}$, nonlinearity coefficient, γ. The pulse width achievable is estimated to be $2c\sqrt{\beta_{2,\text{out}}}/(\overline{A}\omega\sqrt{\beta_{2,\text{in}}})$ [sec].

Table 1 summarizes the formulas for the operations.

5. Applications

In this section, we briefly introduce some interesting applications of the MZM-FCG: 1) generation of picosecond/ femtosecond pulse train, 2) generation of muti-color pulses, 3) other applications, such as arbitrary waveform generation, code/label generation for optical

CDMA. The above-mentioned auto-bias control has not yet been implemented in these experimental demonstrations since the comb generator is stable enough for the lab use; however the auto bias control will practically accelerate realization of these applications.

To simply generate ultra short pulse trains in multi wavelengths is challenging but promising [1]. In future ultra-high-speed communication systems, numbers of optical time-division multiplexed channels should be multiplexed in wavelength domain for increasing transmission capacity, where a multi-color pulse source is inevitable. In photonic measurements, two-color pulses are necessary for the measurement based on pump-probe or four-wave mixing methods, which are useful for characterizing ultrafast phenomena in optical devices or components. Here, we demonstrate two-color pulse generation modifying the former pulse source. The problem in the above-mentioned MZM+SMF method is that the pulse generation is highly wavelength dependent. To cope with this problem, a dispersion-flattened dispersion compensating fiber (DF-DCF) is applied for pulse synthesis. The pulse source exhibits wavelength tunability covering the full range of telecom C band. Two color pulses can be simultaneously generated by injecting two CW sources into the MZM based pulse generator. The optical spectrum obtained from the pulse generator is shown in Fig. 8(a). It is found that two bundles of optical comb were simultaneously generated at around 1550 nm 1560 nm. Fig. 8(b) shows the autocorrelation traces measured when the BPF was tuned at the wavelengths, respectively. From the autocorrelation traces both pulses at 1550 nm and 1560 nm had the pulse width of 4.0 ps and 4.1 ps assuming a Sech2 waveform. Intensity waveform of the generated two-color pulse trains were also characterized with an all-optical sampling oscilloscope. It is found that pulse trains at two different wavelengths were simultaneously generated with a temporal delay of 7 ps. This kind of operation is hardly achieved by conventional mode-locked laser.

In addition to the pulse sources, MZM-FCG offers several attractive applications. For example, MZM-FCG is useful for optical arbitrary waveform generation. Arbitrary waveform can be synthesized by controlling optical amplitude and phase of the generated comb line by line [11][12], which is a key technology for code generation in optical code-division multiplexing systems [12]. Another possibility of the MZM-FCG is application to optical coherence tomography (OCT) [13]. The comb source will be advantageous in constructing fast-scanned OCT.

In conclusion, we have proposed ultra-flat optical frequency comb generation using a conventional dual-drive modulator. We analytically derived the optimal condition required for the comb generation with excellent spectral flatness, which yields a simple formula. The numerical calculations proved that the spectrum of the generated comb is highly flattened under the driving condition. It was also shown that the formula describes the conversion efficency and bandwidth of the generated comb well.

6. References

Arahira, S., Oshiba, S., Matsui, Y., Kanii, T. & Ogawa, Y. (1994). Terahertz-rate optical pulse generation from a passively mode-locked semiconductor laser diode, *Opt. Lett.* 19(11): 834–836.

Jemison, W. (2001). *Microwave Photonics' 01*, pp. 169–172.

Kondo, J., Aoki, K., Kondo, A., Ejiri, T., Iwata, Y., Hamajima, A., Mori, T., Mizuno, Y., Imaeda, M., Kozuka, Y., o. Mitomi & Minakata, M. (2005). High-Speed and Low-Driving-Voltage Thin-Sheet X-cut $LiNbO_3$ Modulator with Laminated Low-Dielectric-Constant Adhesive, *IEEE Photon. Technol. Lett.* 17(10): 2077–2079.

Kourogi, M., Enami, T. & Ohtsu, M. (1994). A Monolithic Optical Frequency Comb Generator, *IEEE Photon. Technol.* 6(22): 214–217.

Margalit, M., Yu, C. & Haus, E. I. H. (1998). Harmonic Mode-Locking Using Regenerative Phase Modulation, *IEEE Photon.Technol.Lett.* 10(3): 337–339.

Morohashi, I., Sakamoto, T., Sotobayshi, H., Hosako, I., Kawanishi, T. & Tsuchiya, M. (2008). Widely repetition-tunable 200fs pulse source using Mach-Zehnder-modulator-based comb generator and dispersion-flattened dispersion-decreasing fiber, *Opt. Lett.* 33(11): 1192–1194.

Morohashi, I., Sakamoto, T., Sotobayshi, H., Hosako, I., Kawanishi, T. & Tsuchiya, M. (2009). Broadband wavelength-tunable ultrashort pulse source using a mach-zehnder modulator and dispersion-flattened dispersion-decreasing fiber, *Opt. Lett.* 34(15): 2297–2299.

Sakamoto, T., Kawanishi, T. & Izutsu, M. (2005). Optoelectronic oscillator using push-pull mach-zehnder modulator biased at null point for optical two-tone signal generation, *Conference on Laser and Electro Optics (CLEO/IQEC2005)*, p. CTuN5.

Sakamoto, T., Kawanishi, T. & Izutsu, M. (2006a). 50-nm wavelength-tunable self-oscillating electro-optic frequency comb generator, *the 2006 Optical Fiber Communication Conference (OFC2006) in Anaheim, California,*.

Sakamoto, T., Kawanishi, T. & Izutsu, M. (2006b). Optoelectronic oscillator using a $linbo_3$ phase modulator for self-oscillating frequency comb generation, *Opt. Lett.* 31(6): 811–813.

Sakamoto, T., Kawanishi, T. & Izutsu, M. (2007a). Asymptotic formalism for ultraflat optical frequency comb generation using a Mach-Zehnder modulator, *Opt. Lett.* 32(11): 1515–1517.

Sakamoto, T., Kawanishi, T. & Izutsu, M. (2007b). Optoelectronic oscillating millimetre-wave generator employing reciprocating optical modulator, *Electron. Lett.* 43(19): 19.

Sakamoto, T., Kawanishi, T. & Izutsu, M. (2008). Widely Wavelength-Tunable Ultra-Flat Frequency Comb Generation Using Conventional Dual-Drive Mach-Zehnder Modulator, *Electron. Lett.* 43(19): 1039–1040.

Sakamoto, T., Kawanishi, T., Shinada, S. & Izutsu, M. (2005). Optoelectronic oscillator using $linbo_3$ intensity modulator with resonant electrode, *Electron. Lett.* 41(12): 716–718.

Sakamoto, T., Morohashi, I. & Kawanishi, T. (2011). Four different principle operation modes for ultra-flat optical comb generation using electro-optic mach-zehnder modulator, *Opt. Lett.* . submitted.

Sugiyama, M., Doi, M., Taniguchi, S., Nakazawa, T. & Onaka, H. (2002). Driver-less 40 Gb/s $LiNbO_3$ modulator with sub-1 V drive voltage, *Optical Fiber Communication Conference (OFC' 02)*, pp. 854–856.

Tsuzuki, K., Kikuchi, H., Yamada, E., Yasaka, H. & Ishibashi, T. (n.d.). 1.3-V_{pp} Push-pull Drive InP Mach-Zehnder Modulator Module for 40 Gbit/s Operation. *31th European Conference on Optical Communication (ECOC 2005)*, Th.2.6.3 , Glasgow, Scotland, Sep, 2005.

Yao, X. & Maleki, L. (1994). High frequency optical subcarrier generator, *Electron. Lett.* 30: 1525–1526.

Yokoyama, H., Hashimoto, Y., Kurita, H. & Ogura, I. (2000). Two-stage all-optical subharmonic clock recovery using modelocked semiconductor lasers, *Electron. Lett.* 36(18): 1577–1578.

Yoshida, E. & Nakazawa, M. (1998). Wavelength tunable 1.0 ps pulse generation in 1.530-1.555 μm region from PLL, regeneratively modelocked fibre laser, *Electron. Lett.* 34(18): 1753–1754.

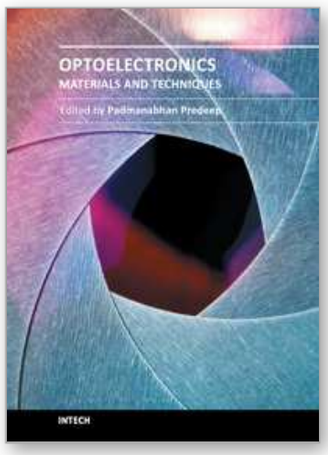

Optoelectronics - Materials and Techniques

Edited by Prof. P. Predeep

ISBN 978-953-307-276-0
Hard cover, 484 pages
Publisher InTech
Published online 26, September, 2011
Published in print edition September, 2011

Optoelectronics - Materials and Techniques is the first part of an edited anthology on the multifaceted areas of optoelectronics by a selected group of authors including promising novices to the experts in the field. Photonics and optoelectronics are making an impact multiple times the semiconductor revolution made on the quality of our life. In telecommunication, entertainment devices, computational techniques, clean energy harvesting, medical instrumentation, materials and device characterization and scores of other areas of R&D the science of optics and electronics get coupled by fine technology advances to make incredibly large strides. The technology of light has advanced to a stage where disciplines sans boundaries are finding it indispensable. Smart materials and devices are fast emerging and being tested and applications developed in an unimaginable pace and speed. Here has been made an attempt to capture some of the materials and techniques and underlying physical and technical phenomena that make such developments possible through some real time players in the field contributing their work and this is sure to make this collection of essays extremely useful to students and other stake holders such as researchers and materials scientists in the area of optoelectronics.

INTECH
open science | open minds

InTech Europe
University Campus STeP Ri
Slavka Krautzeka 83/A
51000 Rijeka, Croatia
Phone: +385 (51) 770 447
Fax: +385 (51) 686 166
www.intechopen.com

InTech China
Unit 405, Office Block, Hotel Equatorial Shanghai
No.65, Yan An Road (West), Shanghai, 200040, China
中国上海市延安西路65号上海国际贵都大饭店办公楼405单元
Phone: +86-21-62489820
Fax: +86-21-62489821

IntechOpen